

Supplementary Material

MTJ Tracking Methods

We estimated AT, muscle, and MTU length changes using previously published MTJ tracking methods (Hoffrén et al., 2012; Lichtwark, 2005; Lichtwark and Wilson, 2006). The ultrasound transducer was placed over the MG-AT MTJ, then securely affixed to the shank using HypaFix® retention tape and ACE bandages (**Fig. 1b**). To approximate AT origin, the characteristic “Y” of the MTJ was manually tracked in each ultrasound image. A calcaneus motion capture marker approximated AT insertion. A custom 3-D printed fixture attached to the transducer allowed tracking of its position and orientation with respect to the lab reference frame. The ultrasound field of view was assumed to be perpendicular to the longitudinal plane of the transducer. AT length was estimated as the straight-line 3D distance from the calcaneus to the MTJ. MG muscle length change was then approximated as the difference between MTU length change (from a regression equation based on ankle and knee angles, Hawkins and Hull, 1990) and AT length change.

MF Tracking Methods

We estimated AT, muscle, and MTU length changes using previously published MF tracking methods (Cronin and Lichtwark, 2013; Farris and Sawicki, 2012; Hoang et al., 2007; Hoffrén et al., 2012; Masaki Ishikawa et al., 2005; M. Ishikawa et al., 2005; Lichtwark et al., 2007; Lichtwark and Wilson, 2006; Sakuma et al., 2011). The transducer was placed over the MG muscle belly, then securely affixed to the shank using HypaFix® retention tape and ACE bandages (**Fig. 1c**). An automated affine flow algorithm was used to estimate time-varying length of an individual MG muscle fascicle (Farris and Lichtwark, 2016). Manual corrections of the fascicle endpoints were made for frames in which the automated calculation did not track the fascicle well, based on visual inspection of a trained researcher. If the fascicle extended beyond the field of view, the endpoint locations were estimated via linear extrapolation (i.e., by extending the lines of the fascicle and aponeuroses beyond the field of view and finding the intersection point). Pennation angle was calculated for each frame as the angle between the superficial fascia and the muscle fascicle. Changes in fascicle length were then corrected for pennation angle to approximate changes in MG muscle length along the muscle’s line of action. AT length change was then estimated as the difference between MTU length change (from a regression equation based on ankle and knee angles, Hawkins and Hull, 1990), and MG length change.

EMG Data Collection & Analysis

EMG data were collected to supplement primary outcome measures, and used to confirm that muscle activity was consistent with loading expectations for each task. Surface EMG sensors (Delsys Trigno) were placed unilaterally on the medial gastrocnemius (MG), lateral gastrocnemius (LG), soleus (SOL), and tibialis anterior (TA). EMG signals were demeaned, high-pass filtered at 150 Hz, rectified, and low-pass filtered at 10 Hz, and then normalized based on the maximum muscle activation magnitude that occurred during the three recorded tasks (Potvin and Brown, 2004; Zelik et al., 2015). The resulting EMG envelopes from each cycle were normalized to 1000 data points (representing 0 to 100% of the cycle). For each task, on a subject-specific basis, EMG envelopes were averaged over five sequential cycles (**Fig.**

S3b). For subjects in which MTJ and MF tracking trials were performed separately, EMG is only reported for the MF tracking trials.

Explanation of Model Expectations for Each Task

Below we summarize the expected behaviors of a common MTU model: a passive linear extension spring (representing the AT and associated aponeurosis) acting in series with an actuator (representing the muscle). In this study the model represents the MG MTU, which spans distally from the calcaneus (heel), posteriorly across the ankle and knee joints, and then connects proximally to the thigh segment. Since experimental tasks were performed slowly (quasi-statically) dynamic effects due to inertia were ignored for this simple model. It was assumed that the extension spring remained linear and did not become slack (see Extended Discussion below on slack length).

The restricted joint calf contraction task is akin to fixing each end of the MTU model, then ramping up/down the actuator force. As force increased, we expected that the actuator would shorten and the series spring would lengthen by an equal magnitude (**Fig. 3a, top row**). Experimentally this task was achieved by affixing a rigid bar above the knee and thigh. All subjects showed activation of the MG, LG, and SOL that was in accordance with muscle forces ramping up and then down (i.e., the loading pattern assumed in order to derive model expectations). All subjects, except one (**Fig. S3b, column 1**), showed negligible TA activation, indicating that antagonistic muscle contraction was not a significant confounding factor. Subjects also exhibited minimal change in ankle angle (**Fig. S3a, column 1**), as expected due to the rigid bar. However, due to soft tissue deformation against the rigid bar, it was not possible to completely restrict joint motion (Bryant et al., 2008; Magnusson et al., 2001). Nonetheless, the simplified model and experiment task were qualitatively consistent, each capturing the same main muscle and tendon length change behaviors.

The ankle DF/PF with foot in air task was modeled by fixing the MTU at the proximal end, hanging a small mass at the distal end, then slowly driving the actuator to lift and lower the mass. With the foot in the air, relatively low AT force was expected, i.e., only force needed to counteract torque due to the mass of the foot about the ankle joint and to overcome any passive resistance from antagonistic MTUs. The mass of the biological foot is about 1 kg and the center of mass of the foot is about 60 mm anterior to the ankle in neutral position. Assuming an anthropometric AT moment arm of about 50 mm (Honert and Zelik, 2016; McCullough et al., 2011), $<<1$ Nm of torque is needed to support the mass of the foot. Passive joint moments have been estimated to be relatively small across a range of ankle angles. For example, passive ankle moments are expected to be <5 Nm at ankle angles $<90^\circ$, and <10 Nm for the maximum dorsiflexion angles reached during this task (based on Silder et al., 2007). Again assuming an anthropometric AT moment arm, AT forces would typically be <100 N, and at most be about 200 N (which is only about 7% of the force experienced by the AT during walking at moderate speed, Bogey et al., 2005). Consistent with the expectation of low loading, EMG from the MG and other plantarflexors was relatively low throughout the entire DF/PF ankle range of motion (**Fig. S3, column 2**). Also, the TA exhibited activity during dorsiflexion beyond neutral, but was inactive during plantarflexion beyond neutral (**Fig. S3b, column 1**). Additional forces due to joint friction were assumed to be negligible, since experiments involved young, healthy subjects. AT stiffness values in literature are on the order of 130-470 N/mm (Kubo et al., 2007, p. 200; Lichtwark, 2005; Maganaris and Paul, 2002; Magnusson et al., 2001; Muraoka et al., 2005). Due to these relatively low forces acting on a relatively stiff tendon, we

expected AT length change to be small (i.e., less than a few mm) throughout the movement cycle of this DF/PF task (**Fig. 3a, middle row**).

Heel raises were modeled by fixing the MTU at one end, with the distal end free to move as the actuator shortened/lengthened under relatively large force. We assumed that there was low loading on the actuator and series spring at the beginning of the cycle, then forces increased. One might intuit that the MTU force profile over the heel raise cycle would increase monotonically (as one lifts up from the flat footed posture), then plateau at some higher force while the heel was off the ground, then decrease force as a person returned back to foot-flat. The AT force profile is actually somewhat more complex: it is double-peaked due to the dynamically-changing moment arm from the ankle joint to the center of pressure (COP), the point of application of the ground reaction force (GRF). Beginning from foot-flat, as the calf muscles increase their force and lift the heels off the ground, the COP shifts anteriorly towards the distal end of the foot, increasing the ankle-to-COP moment arm and causing a peak in AT force. Then, as the foot rotates about the metatarsophalangeal joints, the ankle shifts anteriorly, decreasing the ankle-to-COP moment arm, and reducing the AT force. As the heel lowers, the cycle is reversed creating a second AT force peak. We confirmed this double-peaked force profile experimentally using motion and ground reaction force data (**Fig. S1**). AT moment arm varies slightly with ankle angle and muscle activation level, but for the $\sim 30^\circ$ of ankle plantarflexion during the heel raise task, the AT moment arm is expected to increase by less than 10 mm (Maganaris and Paul, 2000; McCullough et al., 2011). Even with a 10 mm increase in moment arm, the AT force at peak plantarflexion ($\sim 50\%$ cycle) would only be about 15% (~ 110 N) less than that estimated with a constant moment arm. Based on AT stiffness values in literature (Kubo et al., 2007, p. 200; Lichtwark, 2005; Maganaris and Paul, 2002; Magnusson et al., 2001; Muraoka et al., 2005), this reduction in tendon force would reduce tendon length by <1 mm. Regardless of the precise force profile, the key model takeaway is that we would expect the spring to lengthen proportionally with increasing MTU force (**Fig. 3a, bottom row**). For the heel raise task, EMG results confirmed that all subjects increased activation of the MG, LG, and SOL as the heel began lifting off the ground (**Fig. S3b, column 3**), consistent with the model loading expectations summarized above.

Post-Hoc Corrections to AT Length Change Estimate

For most subjects, as they plantarflexed their ankle beyond neutral in the ankle DF/PF task we observed a roughly linear decrease in AT length (**Fig. 3, middle row**). It was initially tempting to use this DF/PF task to derive an AT length change correction factor based on ankle angle to remove this trend; however, this approach may be ill-advised until the source of error is better understood; for reasons summarized below. Numerically, we could approximate a proportional relationship between ankle angle and AT length change (**Fig. 4, left column**) during this low force task, and treat it as a correction factor. We could apply this correction factor, a function of ankle angle, by subtracting it from the AT estimates. As a result, AT length changes would become small throughout the entire DF/PF cycle (qualitatively consistent with model expectations). The correction factor derived from the low force task could also be used to adjust AT length change estimates from the heel raise task (**Fig. 4, right column**). This would shift the AT behavior towards lengthening, which would again make the experimental results more consistent with model expectations. However, this type of post-hoc adjustment to AT length change would also necessitate adjusting our estimate of either the muscle or MTU length change to compensate, in order to ensure that muscle length change plus tendon length change was still

equivalent to overall MTU length change. Presently it is not clear if, or justified why, either the muscle or MTU estimate should be adjusted *post hoc*. Therefore, before applying any such correction factors we advise that it would be prudent to first discern why this AT length change vs. ankle angle trend exists at all. We anticipate that this deeper understanding will inform our conceptual model of MTU dynamics, or motivate specific refinements in the empirical methods used to estimate AT length change.

Extended Discussion of Slack Length & Straight-Line Tendon Assumption

Slackening of the MG and/or AT (Hug et al., 2013, Hoang et al., 2007, Muraoka et al. 2002) have been estimated to occur at about 20-40° of plantarflexion beyond neutral (i.e., at 50-70° in **Fig. 4**), when the ankle is passively rotated. Thus, AT slackening may degrade the accuracy of tendon length estimates during the DF/PF task, a low force ankle rotation task, when ankle angle is less than about 50-70°; highlighting the importance of considering slack length for certain tasks. However, slack length does not seem to explain the substantial tendon shortening (~10 mm) as the ankle plantarflexed from 90° to 70° in the DF/PF task, nor similar shortening reported in prior literature on passive ankle rotation (Csapo et al., 2013). Furthermore, slack length would not seem to explain the shortening observed during heel raises when the MG was actively contracting (**Fig. S3**). Regression-based estimates of overall MTU length (Grieve, 1978; Hawkins and Hull, 1990) are based on cadaver studies, assuming straight-line approximations and that MTU length is only a function of joint angles (Yuen and Orendurff, 2006). Prior studies (Fukutani et al., 2014; Stosic and Finni, 2011), found that when using a linear approximation, the AT appeared to shorten by 3 mm more than when using an estimate that accounted for curvature (for 30° of plantarflexion beyond neutral). However, this 3 mm error was small compared to the 15 mm of AT shortening we observed for a similar 30° of plantarflexion (during ankle DF/PF, **Fig. 3, middle row**). To approximate the effect of curvature on our estimates, we added a virtual waypoint 50 mm posterior to the ankle joint center that rotated with the foot segment. We then used the calcaneus, waypoint, and MTJ positions to calculate a piecewise tendon length. Using this piecewise tendon estimate accounted for less than 40% of the total shortening for both the ankle DF/PF and heel raise task at peak plantarflexion, indicating that curvature alone does not appear to explain the majority of the tendon shortening. Potential confounds discussed above do not reflect a comprehensive list. Other potential estimation issues have been described in prior literature (e.g., Cronin and Lichtwark, 2013; Epstein and Herzog, 2003; Herbert et al., 2011; Zelik and Franz, 2017).

Supplementary Material References

- Bogey, R.A., Perry, J., Gitter, A.J., 2005. An EMG-to-force processing approach for determining ankle muscle forces during normal human gait. *IEEE Trans. Neural Syst. Rehabil. Eng.* 13, 302–310. <https://doi.org/10.1109/TNSRE.2005.851768>
- Bryant, A.L., Clark, R.A., Bartold, S., Murphy, A., Bennell, K.L., Hohmann, E., Marshall-Gradisnik, S., Payne, C., Crossley, K.M., 2008. Effects of estrogen on the mechanical behavior of the human Achilles tendon in vivo. *J. Appl. Physiol.* 105, 1035–1043. <https://doi.org/10.1152/jappphysiol.01281.2007>
- Cronin, N.J., Lichtwark, G., 2013. The use of ultrasound to study muscle–tendon function in human posture and locomotion. *Gait Posture* 37, 305–312. <https://doi.org/10.1016/j.gaitpost.2012.07.024>
- Csapo, R., Hodgson, J., Kinugasa, R., Edgerton, V.R., Sinha, S., 2013. Ankle morphology amplifies calcaneus movement relative to triceps surae muscle shortening. *J. Appl. Physiol.* 115, 468–473. <https://doi.org/10.1152/jappphysiol.00395.2013>
- Epstein, M., Herzog, W., 2003. Aspects of skeletal muscle modelling. *Philos. Trans. R. Soc. B Biol. Sci.* 358, 1445–1452. <https://doi.org/10.1098/rstb.2003.1344>

- Farris, D.J., Lichtwark, G.A., 2016. UltraTrack: Software for semi-automated tracking of muscle fascicles in sequences of B-mode ultrasound images. *Comput. Methods Programs Biomed.* 128, 111–118. <https://doi.org/10.1016/j.cmpb.2016.02.016>
- Farris, D.J., Sawicki, G.S., 2012. Human medial gastrocnemius force–velocity behavior shifts with locomotion speed and gait. *Proc. Natl. Acad. Sci.* 109, 977–982. <https://doi.org/10.1073/pnas.1107972109>
- Fukutani, A., Hashizume, S., Kusumoto, K., Kurihara, T., 2014. Influence of neglecting the curved path of the Achilles tendon on Achilles tendon length change at various ranges of motion. *Physiol. Rep.* 2. <https://doi.org/10.14814/phy2.12176>
- Grieve, D.W., 1978. Prediction of gastrocnemius length from knee and ankle joint posture.
- Hawkins, Hull, M.L., 1990. A Method For Determining Lower Extremity Muscle-Tendon Lengths During Flexion/Extension Movements.
- Herbert, R.D., Clarke, J., Kwah, L.K., Diong, J., Martin, J., Clarke, E.C., Bilston, L.E., Gandevia, S.C., 2011. In vivo passive mechanical behaviour of muscle fascicles and tendons in human gastrocnemius muscle–tendon units. *J. Physiol.* 589, 5257–5267. <https://doi.org/10.1113/jphysiol.2011.212175>
- Hoang, P.D., Herbert, R.D., Todd, G., Gorman, R.B., Gandevia, S.C., 2007. Passive mechanical properties of human gastrocnemius muscle–tendon units, muscle fascicles and tendons in vivo. *J. Exp. Biol.* 210, 4159–4168. <https://doi.org/10.1242/jeb.002204>
- Hoffrén, M., Ishikawa, M., Avela, J., Komi, P.V., 2012. Age-related fascicle–tendon interaction in repetitive hopping. *Eur. J. Appl. Physiol.* 112, 4035–4043. <https://doi.org/10.1007/s00421-012-2393-x>
- Honert, E.C., Zelik, K.E., 2016. Inferring Muscle-Tendon Unit Power from Ankle Joint Power during the Push-Off Phase of Human Walking: Insights from a Multiarticular EMG-Driven Model. *PLOS ONE* 11, e0163169. <https://doi.org/10.1371/journal.pone.0163169>
- Ishikawa, M., Komi, P.V., Grey, M.J., Lepola, V., Bruggemann, G.-P., 2005. Muscle-tendon interaction and elastic energy usage in human walking. *J. Appl. Physiol.* 99, 603–608. <https://doi.org/10.1152/jappphysiol.00189.2005>
- Ishikawa, M., Niemelä, E., Komi, P.V., 2005. Interaction between fascicle and tendinous tissues in short-contact stretch-shortening cycle exercise with varying eccentric intensities. *J. Appl. Physiol.* 99, 217–223. <https://doi.org/10.1152/jappphysiol.01352.2004>
- Kubo, K., Morimoto, M., Komuro, T., Tsunoda, N., Kanehisa, H., Fukunaga, T., 2007. Influences of tendon stiffness, joint stiffness, and electromyographic activity on jump performances using single joint. *Eur. J. Appl. Physiol.* 99, 235–243. <https://doi.org/10.1007/s00421-006-0338-y>
- Lichtwark, G., 2005. In vivo mechanical properties of the human Achilles tendon during one-legged hopping.
- Lichtwark, G.A., Bougoulias, K., Wilson, A.M., 2007. Muscle fascicle and series elastic element length changes along the length of the human gastrocnemius during walking and running. *J. Biomech.* 40, 157–164. <https://doi.org/10.1016/j.jbiomech.2005.10.035>
- Lichtwark, G.A., Wilson, A.M., 2006. Interactions between the human gastrocnemius muscle and the Achilles tendon during incline, level and decline locomotion. *J. Exp. Biol.* 209, 4379–4388. <https://doi.org/10.1242/jeb.02434>
- Maganaris, C.N., Paul, J.P., 2002. Tensile properties of the in vivo human gastrocnemius tendon. *J. Biomech.* 35, 1639–1646. [https://doi.org/10.1016/S0021-9290\(02\)00240-3](https://doi.org/10.1016/S0021-9290(02)00240-3)
- Maganaris, C.N., Paul, J.P., 2000. In vivo human tendinous tissue stretch upon maximum muscle force generation. *J. Biomech.* 33, 1453–1459. [https://doi.org/10.1016/S0021-9290\(00\)00099-3](https://doi.org/10.1016/S0021-9290(00)00099-3)
- Magnusson, S.P., Aagaard, P., Rosager, S., Dyhre-Poulsen, P., Kjaer, M., 2001. Load-displacement properties of the human triceps surae aponeurosis in vivo. *J. Physiol.* 531, 277–288. <https://doi.org/10.1111/j.1469-7793.2001.0277j.x>

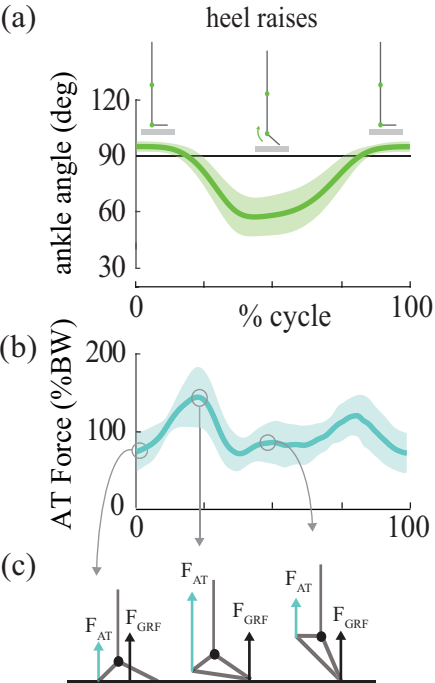
- McCullough, M.B.A., Ringleb, S.I., Arai, K., Kitaoka, H.B., Kaufman, K.R., 2011. Moment Arms of the Ankle Throughout the Range of Motion in Three Planes. *Foot Ankle Int.* 32, 300–306. <https://doi.org/10.3113/FAI.2011.0300>
- Muraoka, T., Muramatsu, T., Fukunaga, T., Kanehisa, H., 2005. Elastic properties of human Achilles tendon are correlated to muscle strength. *J. Appl. Physiol.* 99, 665–669. <https://doi.org/10.1152/jappphysiol.00624.2004>
- Potvin, J.R., Brown, S.H.M., 2004. Less is more: high pass filtering, to remove up to 99% of the surface EMG signal power, improves EMG-based biceps brachii muscle force estimates. *J. Electromyogr. Kinesiol.* 14, 389–399. <https://doi.org/10.1016/j.jelekin.2003.10.005>
- Sakuma, J., Kanehisa, H., Yanai, T., Fukunaga, T., Kawakami, Y., 2011. Fascicle–tendon behavior of the gastrocnemius and soleus muscles during ankle bending exercise at different movement frequencies. *Eur. J. Appl. Physiol.* 112, 887–898. <https://doi.org/10.1007/s00421-011-2032-y>
- Silder, A., Whittington, B., Heiderscheid, B., Thelen, D.G., 2007. Identification of passive elastic joint moment–angle relationships in the lower extremity. *J. Biomech.* 40, 2628–2635. <https://doi.org/10.1016/j.jbiomech.2006.12.017>
- Stosic, J., Finni, T., 2011. Gastrocnemius tendon length and strain are different when assessed using straight or curved tendon model. *Eur. J. Appl. Physiol.* 111, 3151–3154. <https://doi.org/10.1007/s00421-011-1929-9>
- Yuen, T.J., Orendurff, M.S., 2006. A comparison of gastrocnemius muscle–tendon unit length during gait using anatomic, cadaveric and MRI models. *Gait Posture* 23, 112–117. <https://doi.org/10.1016/j.gaitpost.2004.12.007>
- Zelik, K.E., Franz, J.R., 2017. It’s positive to be negative: Achilles tendon work loops during human locomotion. *PLOS ONE* 12, e0179976. <https://doi.org/10.1371/journal.pone.0179976>
- Zelik, K.E., Scaleia, V.L., Ivanenko, Y.P., Lacquaniti, F., 2015. Coordination of intrinsic and extrinsic foot muscles during walking. *Eur. J. Appl. Physiol.* 115, 691–701. <https://doi.org/10.1007/s00421-014-3056-x>

Figure Captions

Fig. S1. Heel raise kinematics and kinetics. (a) Ankle angle vs. movement cycle. (b) Estimated AT force vs. movement cycle. AT force (F_{AT}) was estimated by dividing ankle moment (from standard inverse dynamics) by AT moment arm about the ankle and expressed as percentage of body weight (%BW). Depicted are inter-subject means and standard deviations (shaded regions). (c) Simplified moment balance about the ankle joint. The double-peaked AT force profile occurs because the AT has a roughly constant moment arm about the ankle whereas there is a dynamically-changing moment arm from the ankle to the center of pressure (the point of application of the ground reaction force, F_{GRF}).

Fig. S2. Subject-specific results. AT (thick blue), MG muscle (dashed red) and MTU (thin black) length changes vs. movement cycle. Major columns are tasks. Unshaded columns show the MTJ method results and shaded columns show the MF method results. The top row represents the mean and standard deviation across subjects. Remaining rows each represent subject-specific average results.

Fig. S3. Kinematics and subject-specific EMG. (a) Ankle (solid green) and knee (dashed green) joint angles vs. movement cycle, averaged across eight subjects. (b) Medial gastrocnemius (MG, red), lateral gastrocnemius (LG, green), soleus (SOL, blue), and tibialis anterior (TA, orange), muscle activation vs. movement cycle. EMG magnitudes are reported as a percentage of the maximum activation observed during these three tasks. Each column is a task. Each row represents subject-specific average results.



restricted joint

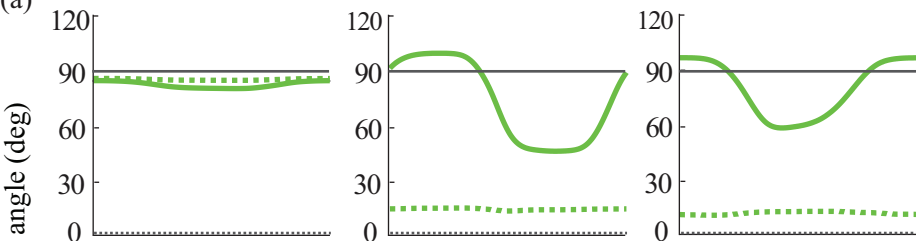
ancke DF/PF

heel raises

— ANKLE

- - - KNEE

(a)



(b)

MG

LG

SOL

TA

